Gradual Faults Diagnosis by a Novel Impedance Characterization Method

Najwa Lamdihine, Mohammed Ouassaid, and Ghassane Aniba

Engineering for Smart & Sustainable Systems Research Center
Mohammadia School of Engineers (EMI), Mohammed V University in Rabat, Morocco
najwa.lamdihine@research.emi.ac.ma,{ouassaid,ghassane}@emi.ac.ma

2021 12th International Renewable Engineering Conference (IREC) | 978-1-6654-2548-3/20/$31.00 ©2021 IEEE | DOI: 10.1109/IREC51415.2021.9427860

***Abstract*—This paper presents a novel photovoltaic impedance characterization method aiming to evaluate the state and gradual decrease of photovoltaic (PV) panel health. The big challenge to meet for the PV panels is to guarantee their robust and reliable functioning, and specially maintain their efficient yield as long as possible, which imply that a real-time diagnose is mandatory to detect rapidly the faults that may occur on PV plants and then react effectively. This study developed a novel method that allows not only to detect, locate and recognize the type of PV defects on an already installed PV plant, but also to measure the discordance between the manufacturer PV datasheet and the real performance of the PV panel once received from the supplier. The impedance characterization is a new analytical and criterion method that uses the Photovoltaic Plant Reflectometry Profile (PPRP) in order to measure exactly any discordance between an ideal state PV module and a defective one, and, even detect multiple faults in a string of connected PV modules. Simulation results show that the proposed method is a valid one that detects any type of PV faults.**

***Index Terms*—Defects diagnosis; Transmission lines; Photovoltaic Plant Reflectometry Profile; Renewable energy; Impedance Characteristic**

I. Introduction

NOWADAYS the energy needs of humanity are experiencing a flagrant increase by dint of massive industrialization, demographic evolution and the development of certain geographical areas which negatively impacts the balance of the earth's atmosphere by increasing the greenhouse effect. Therefore, the adoption of clean and non-polluting green energies is one of the most important solutions to this dilemma. In fact, the use of renewable energies such as solar energy will gradually reduce greenhouse gas emissions in industrialized countries while in developing countries it will untie the isolation from remote areas by allowing them access to energy services which will lead to limit the dependence of these countries on fossil energy resources.

The use of photovoltaic (PV) panels, as grid connected or standalone power systems, is only profitable if a satisfactory efficiency is achieved. However, in most of the cases both configurations cited above are sensitive to the vagaries of PV module performance caused by various reasons such as partial shading, partial or total opacity of the panels in the absence of cleaning, local failures or aging of PV cells. Actually, the presence of a fault is only detected in hindsight, when the energy balance turns out to be lower than forecasts for a given period, hence, the average energy efficiency of the photovoltaic installation can be significantly and definitively reduced if the fault is not quickly detected and corrected [1]. On the other hand, the existence of PV hot spots or electrical discontinuities, resulting from electrical and thermal faults, are not easy to detect and often require the intervention of a specialist with costly equipment. In addition, the absence of maintenance reduces the immunity of those installations against these faults, which on the end will undoubtedly lead to their total unavailability. It is evident that the reduction of PV installations profitability represents a spoiler for the advancement of this technology, which is already subdued by the low yield of the current photovoltaic cells, even though the solar energy potential is significant. Hence, it is important to develop an efficient fault diagnosis technique able to detect, locate and recognize the exact fault type. In literature, plenty of failure detection techniques have been developed and classified depending on the category of the PV failure targeted. Indeed, visual detection techniques are sufficient for failures such as yellowing, delimitation, bubbles, cell cracks, misalignment, burnt cells, dust and soiling [2]. Furthermore, in the case of thermal defects like hot spot formation, infrared image techniques are used alone [3], or combined with other algorithms such as simple linear iterative clustering (SLIC) [4]. In addition, for more dangerous and critical PV faults class, which regroups the electrical defects, other advanced techniques have been proposed such as neural networks [5], Spread-spectrum time domain reflectometry (SSTDR) [6]. In reference [7], authors are interested in ground and line to line fault detection using Perturb and observe (P&O) maximum power point tracker (MPPT) algorithm, and the works in [8], [9] are based respectively on multi-resolution signal decomposition technique to detect short-circuit faults and multistage morphological algorithm arc fault detector.

This paper presents an impedance characterization method able to locate any fault type and compute the exact impedance value of the faulty module, then, deduce the cause of the defect. In fact, it is based on the photovoltaic plant reflectometry profile (PPRP) technique [10], [11] that rests on the comparison between the defective and the ideal PPRP, after that, a curve fitting to the PPRP model is used in order to compute the impedance values of the different modules on a PV string.

Section II presents the theoretical basics used in this study. Section III describes the proposed impedance characterization

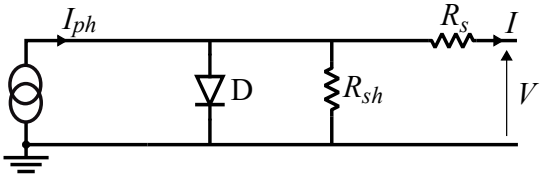

Fig. 1. Equivalent circuit of a solar cell

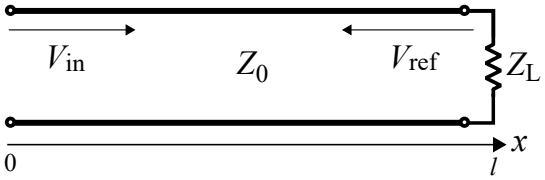

Fig. 2. Simple transmission line model

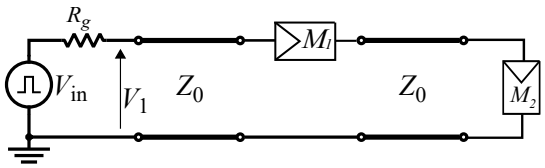

Fig. 3. PV system with two PV modules and transmission lines

method, then simulation and results are given in Section IV, followed by conclusions in Section V.

II. Background Concepts

Each PV array comprises multiple PV modules wired in series and parallel to achieve the desired voltage and current, where each PV module is an assembly of N interconnected solar cells embedded between front and back sheets and encapsulated to guarantee their protection from harsh environment. It is important to note that solar cells are considered as the fundamental building blocks of PV systems. To better understand the electronic behavior of those blocks, an equivalent circuit of a solar cell is given in Fig. 1, which is composed of a current source in parallel with a diode, however, for the reason that no solar cell is ideal, resistive components that models the power losses have been added to the model, manifested by the shunt resistance R_{sh}, which represents the poor solar cell design and manufacturing defects, and by the series resistance R_{s} which models three effects: the contact resistance between the metal contact and the silicon, the movement of current through the emitter and base of the solar cell, and, the resistance of the top and rear metal contacts. The PPRP presented in [10], [11] is a new analytical technique which is based on sending a negative pulse signal through photovoltaic panels considered as a load since there is no solar irradiance, and record via an oscilloscope the reflected signal at the entrance of the line which will be analyzed and compared to the ideal one computed analytically using the PV datasheet in order to detect and locate any impedance change. The transmission line propagation theory [12] contributed a lot in the development of the mathematical part of this technique by offering a simplified model of transmission line drawn in Fig. 2 where Z_0 is the characteristic impedance of the line, and Z_{L} is the load impedance. In this model, the division of the reflected signal amplitude V_{ref} by the incident signal amplitude V_{in} allows to calculate the reflection coefficient ρ expressed in (1). Another important parameter is the round trip time (RTT) noted here by Δt. In fact, in case of an impedance mismatch characterized by $Z_{\text{L}} \neq Z_0$ through the transmission line, the time delay Δt between the transmission of the incident wave and the reception of the reflected wave is given by (2) where v is the propagation speed, and l is the length of the line. This equation represents the key behind the capability to locate the position of a PV defect.

$$\rho = \frac{Z_{\text{L}} - Z_0}{Z_{\text{L}} + Z_0} = \frac{V_{\text{ref}}}{V_{\text{in}}}, \tag{1}$$

$$\Delta t = \frac{2l}{v}. \tag{2}$$

Every healthy PV module has a specific impedance between its pair nodes, and similarly, the most often degradation forms that occur on PV installations such as micro or latent cracks, insulation degradation, line to line fault, ground fault and open/short circuit have specific impedance values different from the healthy PV module initial impedance value. Therefore, the impedance characterization method can promptly recognize the type of the PV defect, unlike most of the other proposed techniques in literature that are limited to detecting the existence of the defect without specifying its type.

III. Impedance Characterization Method

In [10] the PPRP technique was applied in the case of two PV modules M_1, M_2 connected in series without the presence of the by-pass diodes as depicted in Fig. 3. The modules are regarded as a load for the reason that the test is done at night which means zero PV power generation, thus, each PV module can be modeled as an impedance R_{c} equal to the number of solar cells N that construct it multiplied by the sum of the shunt resistance R_{sh} and the series resistance R_{s} [1], as shown in (3), which justifies the equivalence between Fig. 3 and Fig. 4.

$$R_{\text{c}} = N(R_{\text{s}} + R_{\text{sh}}) \tag{3}$$

Moreover, in [10] the PPRP technique was used mainly to calculate the response of a healthy PV system named "ideal PPRP" which will serve later as a baseline for comparison, in order to detect any defective module. Herein, and as a first contribution, the PPRP has been generalised, it is no longer limited to the calculation of the ideal response only. Henceforth, it is able to calculate the response of any module including the defective ones, the new results are presented in Tab. I where ρ_1 and ρ_2 represent the reflection coefficients at the level of the first and the second PV modules, respectively. They are expressed in function of equivalent module impedances R_{c_1} , R_{c_2} in (4) and (5), in addition to β, α given in (6), (7) where R_{g} is the internal resistance of the pulse generator and Z_0 is the characteristic impedance of the transmission line. Indeed, R_{g} has been chosen equal to Z_0 so as to have an adapted line at the entrance of transmission line, $R_{\text{g}} = Z_0 = 50\Omega$ -

[1] R_{s} and R_{sh} can be calculated from the datasheet parameters as indicated in [13]

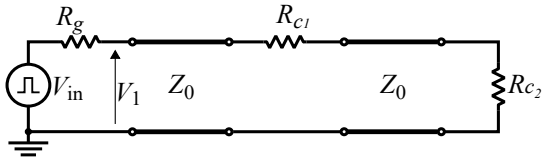

Fig. 4. Equivalent electric schematic of the PV system

TABLE I
GENERALIZED PPRP IN THE CASE OF TWO PV MODULES

Index (i)	Time	Voltage V_1
1	$0 \leq t < 2\tau$	βV_{in}
2	$2\tau \leq t < 4\tau$	$\beta(1+\rho_1)V_{\text{in}}$
3	$4\tau \leq t < 6\tau$	$\beta(1+\rho_1)[1+\alpha_1^2\rho_2(1+\rho_1)]V_{\text{in}}$
4	$6\tau \leq t$	$\beta(1+\rho_1)[1+\alpha_1^2\rho_2(1+\rho_1)[1+\rho_1\rho_2]]V_{\text{in}}$

$$\rho_1 = \frac{R_{\text{c}_1}}{2Z_0 + R_{\text{c}_1}}, \tag{4}$$

$$\rho_2 = \frac{R_{\text{c}_2} - Z_0}{R_{\text{c}_2} + Z_0}, \tag{5}$$

$$\beta = \frac{Z_0}{Z_0 + R_{\text{g}}} = \frac{1}{2}, \tag{6}$$

and,

$$\alpha_1 = \frac{Z_0}{Z_0 + R_{\text{c}_1}}. \tag{7}$$

The second contribution of this paper is the use of the field test curve fitting to the PPRP model in order to calculate the equivalent impedance of the doubtful modules then compare it with the correct one computed using the datasheet parameters. This approach will allow the detection of any gradual impedance change that occurs in the PV modules. Hence, to reach that objective, a development of mathematical equations that links the equivalent PV module impedance and the voltage V_1 characterizing the PPRP model is required. However, as it appears on Tab. I, the voltage V_1 changes with time, and for each time interval $i = 1, 2, 3, \ldots$, the PV module impedance value is deduced from the equation that corresponds to that interval. For instance, in interval index 2, the coefficient ρ_1 can be easily deduced in function of the voltage $V_1(2)$ as shown in (8), and by developing (4), a direct expression of R_{c_1} in function of ρ_1 is presented in (9). So the knowing of the reflection coefficient ρ_1 will automatically lead to the determination of the value of the first PV module impedance R_{c_1}. Fig. 5 shows the variation of the impedance R_{c_1} in function of $V_1(2)/V_{\text{in}}$.

$$\rho_1 = \frac{V_1(2)}{\beta V_{\text{in}}} - 1 \tag{8}$$

$$R_{\text{c}_1} = \frac{2Z_0\rho_1}{1-\rho_1} \tag{9}$$

In like manner, during the time interval index 3, the coefficient ρ_2 can be inferred in terms of $V_1(3)$ as revealed in (10) and by the same logic, the development of (5) help to find R_{c_2} as expressed in (11). Hence, the knowledge of ρ_2 permits directly the deduction of the second PV module impedance value R_{c_2}. Fig. 6 shows the variation of the impedance R_{c_2} in terms of $V_1(2)/V_{\text{in}}$ and $V_1(3)/V_{\text{in}}$.

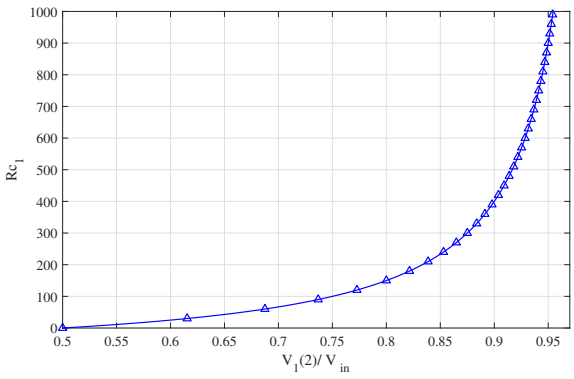

Fig. 5. Variation of R_{c_1} in terms of $V_1(2)/V_{\text{in}}$

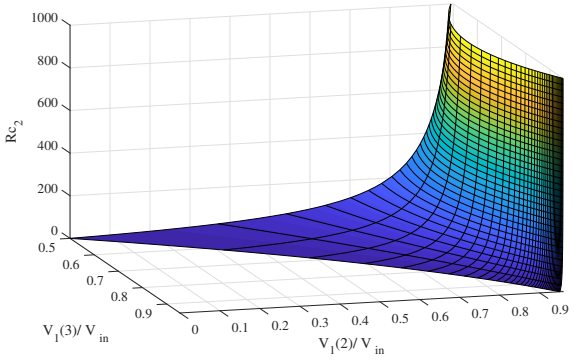

Fig. 6. Variation of R_{c_2} in terms of $V_1(2)/V_{\text{in}}$ and $V_1(2)/V_{\text{in}}$

$$\rho_2 = \frac{\frac{V_1(3)}{\beta(1+\rho_1)V_{\text{in}}} - 1}{\alpha_1^2(1+\rho_1)} \tag{10}$$

$$R_{\text{c}_2} = Z_0\frac{1+\rho_2}{1-\rho_2} \tag{11}$$

In the light of this study, and as a first advantage of this method, consider two defect's scenarios: short and open circuits.

1) *First PV module M_1 short-circuited (SC):* Having a short circuit at the level of the first module means that the equivalent impedance of that module R_{c_1} is equal to 0 and replacing it with this value in (4) and (7), respectively. The reflection coefficient ρ_1 will be equal to 0, α_1 to 1, thereupon, the voltage $V_1(2)$ will take the value βV_{in} rely on (8). Practically, the voltage $V_1(2)$ in the time interval index 2 will keep the same value of the previous time interval index 1.
2) *First PV module M_1 open-circuited (OC):* While having M_1 open-circuited, the value of R_{c_1} will tend towards ∞, and using the same equations (4) and (7), ρ_1 takes the value 1, and α_1 takes the value 0, consequently, by means of (8), the voltage $V_1(2)$ is then equal to $2\beta V_{\text{in}}$, in a word, a full reflection will take place in that case.
3) *Second PV module M_2 short-circuited:* Considering M_1 non defective, if M_2 is short-circuited then $R_{\text{c}_2} = 0$, hence using (5) $\rho_2 = -1$, thus, according to (10) the voltage $V_1(3) = [1 - \alpha_1^2(1+\rho_1)]\beta(1+\rho_1)V_{\text{in}}$.

TABLE II
BORDERLINE FAULT CASES

M_1	M_2	α_1	ρ_1	ρ_2	$V_1(2)$	$V_1(3)$
SC	SC	1	0	-1	βV_{in}	0
SC	OC	1	0	1	βV_{in}	$2\beta V_{\text{in}}$
OC	SC	0	1	-1	$2\beta V_{\text{in}}$	$2\beta V_{\text{in}}$
OC	OC	0	1	1	$2\beta V_{\text{in}}$	$2\beta V_{\text{in}}$

TABLE III
STC PARAMETERS OF THE TESTED PV MODULE

Parameters	Value
Cell Type	Poly-crystalline 156×52 mm
No. of Cells (N)	42 (6×7)
Weight	7.0 Kg
Peak Power (Pmax)	50 Wc
Open Circuit Voltage (Voc)	24.8 V
Short Circuit Current (Isc)	2.7 A
Maximum Power Voltage (Vmp)	21 V
Maximum Power Current (Imp)	2.39 A
Shunt Resistor per solar cell R_{sh}	2.562
Serial Resistor per solar cell R_{s}	0.005
Operating and Storage Temperature	$-40 \sim +85°\text{C}$

4) *Second PV module M_2 open-circuited:* As the previous case, M_1 is considered non defective, M_2 is open circuited, which implies $R_{\text{c}_2} = \infty$, and by means of (5) $\rho_2 = 1$, then, using (10) $V_1(3) = [1 + \alpha_1^2(1 + \rho_1)]\beta(1 + \rho_1)V_{\text{in}}$.

In the final analysis, once the voltage V_1 takes one of the values cited above, depending on the considered tie interval index i, a direct deduction of the location and the type of fault can be easily done.

In fact, the impedance characterization method is not limited to the detection of single faults, it is widened to detect multiple faults that may occur simultaneously in both PV modules. Mathematical results summarizing the combination between open and short-circuit fault scenarios, in the case of two PV modules M_1 and M_2 are presented in Tab. II.

IV. SIMULATION AND RESULTS

In order to study the performance of the proposed impedance characterization method to detect and identify a PV defect type, simulations were conducted using two PV modules owning the standard test conditions (STC) datasheet parameters presented in Tab. III in addition to the numerical values of the used pulse generator and transmission line factors, given in Tab. IV.

Indeed, the principle of this simulation is based firstly, on computing the ideal PPRP using the mathematical equations in Tab. I, coupled with (4), (5), (6), (7) and (3), besides the PV datasheet parameters. Secondly, it consists of a first scenario on the creation of a defect in the first PV module M_1 and considering a healthy second PV module M_2, then the pulse generator is used to send a negative pulse through the PV modules in order to measure the corresponding PPRP named "defective PPRP". Finally, a curve fitting of the voltage values corresponding to the interval where the ideal and defective PPRP are no longer superimposed, combined with (8) and (9), are used to determine the new value of the first PV module impedance resulting from the fault created within it.

TABLE IV
NUMERICAL VALUES OF SIMULATION

	Parameters	value
Pulse generator	V_{in}	$-70V$
	Sample time	0.1ns
	R_{g}	50Ω
Transmission line	Z_0	50Ω
	Delay time τ	5ns

TABLE V
NUMERICAL VALUES OF V_1 IN CASE OF FIRST PV MODULE DEFECT

index (i)	Time Intervals	Voltage V_1
1	$0 \leq t < 2\tau$	-35
2	$2\tau \leq t < 4\tau$	-56.9
3	$4\tau \leq t < 6\tau$	-58.7
4	$6\tau \leq t$	-59.1

One of the major power drop origins in PV fields is the Fill Factor (FF) decrease, mainly caused by the increase of the series resistance R_{s} resulting from solar cells solder bond degradation. A first simulation case that consists on raising the value of R_{s} of the first PV module M_1 to generate a fault is conducted. Results are presented in Fig. 7 where ideal PPRP and defective PPRP present the response of a healthy and defective system, respectively. This figure shows that, from the time interval index 2, the curves start to differentiate. This indicates the presence of an anomaly within the first PV module. However, to determine the new value of R_{c_1} following the created fault, the new value of the voltage V_1 for each time interval should be known, therefore a direct extraction of these values is done using the pace of the defective PPRP which reveals the numerical values resumed in Tab. V, and by replacing $V_1(1)$ by its value in (8), and (9), the value of R_{c_1} is then calculated and it is equal to 167.16Ω. Nevertheless, when replacing $V_1(2)$ by its value in (10) and (11), the R_{c_2} is found equal to 107.181Ω, which is the same value as the healthy PV module equivalent impedance R_{cs}, computed based on datasheet parameters. This demonstrates that the first PV module is defective, whereas the second PV module is healthy. Thereby, a PV fault detection, location and calculation of the resulting defective impedance has been successfully done using the impedance characterization method.

However, the PV power production is not only affected by high values of series resistance R_{s} but also by low shunt resistance R_{sh} values that provides an alternate current path for the light generated current, which leads to an increase of the leakage current that lowers the maximum output PV power. Therefore, a second simulation scenario is performed similar to the first one with the difference which is the reduction of R_{sh} of the second PV module M_2 while considering a healthy first PV module. Fig. 8 shows in this case that the discordance between the two curves starts from the time interval index 3 which denotes the presence of a defect in the second PV module. In the same manner, the extraction of $V_1(3)$ value from the defective PPRP pace coupled with (10) and (11) determines $R_{\text{c}_2} = 69.06\Omega \neq R_{\text{cs}}$, albeit $R_{\text{c}_1} = 107.181\Omega = R_{\text{cs}}$, then again the impedance characterization method has demonstrated its effectiveness. In a third simulation scenario,

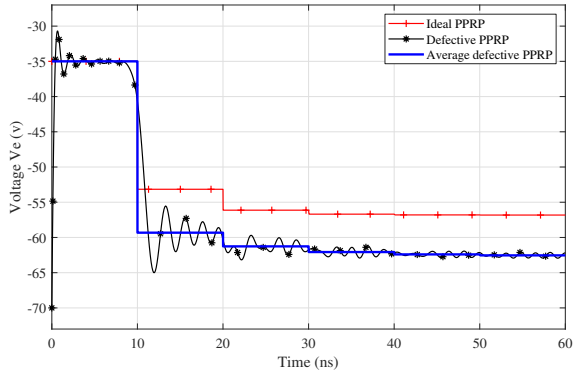

Fig. 9. PPRPs in a scenario with defects on both PV modules

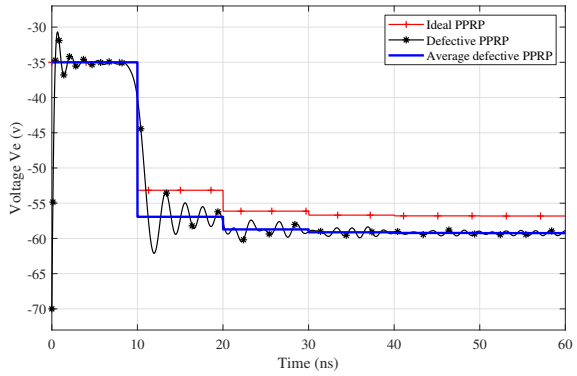

Fig. 7. PPRPs in a scenario with defects on the first PV module M_1

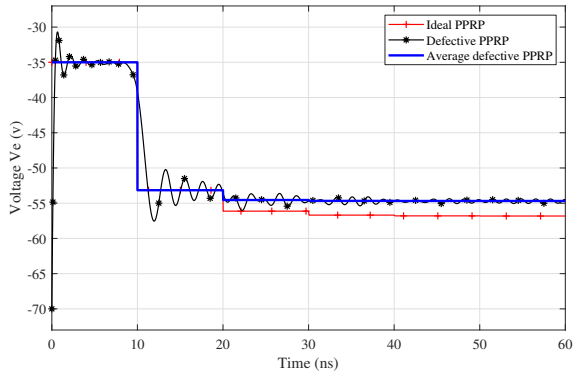

Fig. 8. PPRPs in a scenario with defects on the second PV module M_2

a multiple PV defects were emulated, where both the first and second PV modules M_1, M_2 are defectives. Results are presented in Fig. 9 and identically to the previous scenarios, the values of the voltage V_1 extracted from the defective PPRP during time interval indexes 2 and 3 coupled with equations (8), (9), (10) and (11) allows the calculation of the impedances R_{c_1} and R_{c_2} which are equal to 227.01Ω and 208.13Ω, respectively. As it can be seen, both R_{c_1} and R_{c_2} have totally different values from the healthy PV module equivalent impedance R_{cs} which confirms the presence of failures within both PV modules M_1 and M_2. Actually, the different impedance values characterizing the defective PV modules used in the three simulation scenarios can be a result of many microscopic degradation mechanisms that deteriorates PV modules, like thermomechanical depletion, cracks develop or even emitter layer pinholes, not to mention the problems linked to PV connections abrasion. In essence, the impedance characterization method together with the PPRP technique have substantiated their ability to foremost detect any impedance change within the PV installations even the smallest ones, then locate the defective PV module and at last calculate the exact value of the faulty PV impedance permitting, hence, the recognition of the occurred PV defect type.

V. Conclusion

This paper presents a new impedance characterization method aiming not only to detect or locate flaws and defects that occurs in a large scale PV array, but also to determinate the type of this defect. The latter is achieved by computing the equivalent impedance of the defective PV module either in case of the well-known PV defects such as open/short circuit or in case of the less-known defects such as snail tracks, cells cracks or bubbles, delamination or manufacturing defects. Adjacent to its effectiveness and accuracy, this method has the advantage of simplicity and doesn't require neither specialized equipment nor an expert technician to make the tests.

References

[1] F. Spertino, E. Chiodo, A. Ciocia, G. Malgaroli, and A. Ratclif, "Maintenance Activity, Reliability Analysis and Related Energy Losses in Five Operating Photovoltaic Plants," in *2019 IEEE International Conference on Environment and Electrical Engineering and 2019 IEEE Industrial and Commercial Power Systems Europe (EEEIC / I&CPS Europe)*. Genova, Italy: IEEE, Jun. 2019, pp. 1–6.

[2] W. Chine, A. Mellit, V. Lughi, A. Malek, G. Sulligoi, and A. Massi Pavan, "A novel fault diagnosis technique for photovoltaic systems based on artificial neural networks," *Renewable Energy*, vol. 90, pp. 501–512, 2016.

[3] M. Islam, G. Hasan, I. Ahmed, M. Amin, S. Dewan, and M. M. Rahman, "Infrared Thermography Based Performance Analysis of Photovoltaic Modules," in *2019 International Conference on Energy and Power Engineering (ICEPE)*. Dhaka, Bangladesh: IEEE, Mar. 2019, pp. 1–5.

[4] M. Alsafasfeh, I. Abdel-Qader, and B. Bazuin, "Fault detection in photovoltaic system using SLIC and thermal images," in *2017 8th International Conference on Information Technology (ICIT)*. Amman, Jordan: IEEE, May 2017, pp. 672–676.

[5] S. Rao, A. Spanias, and C. Tepedelenlioglu, "Solar Array Fault Detection using Neural Networks," in *2019 IEEE International Conference on Industrial Cyber Physical Systems (ICPS)*. Taipei, Taiwan: IEEE, May 2019, pp. 196–200.

[6] M. U. Saleh, C. Deline, S. Kingston, N. K. T. Jayakumar, E. Benoit, J. B. Harley, C. Furse, and M. Scarpulla, "Detection and Localization of Disconnections in PV Strings Using Spread-Spectrum Time-Domain Reflectometry," *IEEE Journal of Photovoltaics*, vol. 10, no. 1, pp. 236–242, Jan. 2020.

[7] D. S. Pillai and N. Rajasekar, "An MPPT-Based Sensorless Line–Line and Line–Ground Fault Detection Technique for PV Systems," *IEEE Transactions on Power Electronics*, vol. 34, no. 9, pp. 8646–8659, Sep. 2019.

[8] Z. Yi and A. H. Etemadi, "Fault Detection for Photovoltaic Systems Based on Multi-Resolution Signal Decomposition and Fuzzy Inference Systems," *IEEE Transactions on Smart Grid*, vol. 8, no. 3, pp. 1274–1283, May 2017.

[9] M. Kavi, Y. Mishra, and M. Vilathgamuwa, "DC Arc-Fault Detection in PV Systems Using Multistage Morphological Fault Detection Algorithm," in *IECON 2018 - 44th Annual Conference of the IEEE Industrial Electronics Society*. D.C., DC, USA: IEEE, Oct. 2018, pp. 1746–1751.

[10] N. Lamdihine, M. Ouassaid, and G. Aniba, "A Novel Gradual Faults Diagnosis Using the Photovoltaic Plant Reflectometry Profile," in *2018 IEEE PES Innovative Smart Grid Technologies Conference Europe (ISGT-Europe)*. Sarajevo, Bosnia and Herzegovina: IEEE, Oct. 2018, pp. 1–5.

[11] ——, "A Dual PV Panel Defects Diagnosis Using the Photovoltaic Plant Reflectometry Profile," in *2018 Renewable Energies, Power Systems & Green Inclusive Economy (REPS-GIE)*. Casablanca: IEEE, Apr. 2018, pp. 1–5.
[12] D. Pozar, *Microwave Engineering*, 4th ed., ser. Addison-Wesley Series in Electrical and Computer Engineering. Wiley, Dec. 2011.
[13] A. A. E. Tayyan, "Turkish Journal of Physics A simple method to extract the parameters of the single-diode model of a PV system," *Turkisch Journal of Physics*, vol. 37, pp. 121–131, 2013.